Macular Layer Thickness and Effect of BMI, Body Fat, and Traditional Cardiovascular Risk Factors: The Tromsø Study

Therese von Hanno,[1,2] Live Lund Hareide,[3] Lars Småbrekke,[4] Bente Morseth,[5] Monica Sneve,[6,7] Maja Gran Erke,[7,8] Ellisiv Bøgeberg Mathiesen,[2,9] and Geir Bertelsen[10,11]

[1]Department of Ophthalmology, Nordland Hospital Trust, Bodø, Norway
[2]Department of Clinical Medicine, UiT The Arctic University of Norway, Tromsø, Norway
[3]Faculty of Medicine, University of Oslo, Oslo, Norway
[4]Department of Pharmacy, UiT The Arctic University of Norway, Tromsø, Norway
[5]School of Sport Sciences, UiT The Arctic University of Norway, Tromsø, Norway
[6]Hospital Administration, Bærum Hospital, Vestre Viken Hospital Trust, Bærum, Norway
[7]Department of Ophthalmology, Oslo University Hospital, Oslo, Norway
[8]Directorate of eHealth, Oslo, Norway
[9]Department of Neurology, University Hospital of North Norway, Tromsø, Norway
[10]Department of Ophthalmology, University Hospital of North Norway, Tromsø, Norway
[11]Department of Community Medicine, UiT The Arctic University of Norway, Tromsø, Norway

Correspondence: Therese von Hanno, Therese von Hanno, Department of Ophthalmology, Nordland Hospital Trust, Bodø 8092, Norway;
therese.von.hanno@uit.no.

Received: April 22, 2022
Accepted: July 25, 2022
Published: August 12, 2022

Citation: von Hanno T, Hareide LL, Småbrekke L, et al. Macular layer thickness and effect of BMI, body fat, and traditional cardiovascular risk factors: The Tromsø Study. *Invest Ophthalmol Vis Sci.* 2022;63(9):16.
https://doi.org/10.1167/iovs.63.9.16

Purpose. The purpose of this study was to investigate associations between cardiovascular risk factors and the thickness of retinal nerve fiber layer (RNFL), ganglion cell-inner plexiform layer (GCIPL), and outer retina layers (ORL).

Methods. In this population-based study, we included participants from the Tromsø Study: Tromsø6 (2007 to 2008) and Tromsø7 (2015 to 2016). Persons with diabetes and/or diagnosed glaucoma were excluded from this study. Retinal thickness was measured on optical coherence tomography (Cirrus HD-OCT) macula-scans, segmented on RNFL, GCIPL, and ORL and associations were analyzed cross-sectionally ($N = 8288$) and longitudinally ($N = 2595$). We used directed acyclic graphs (DAGs) for model selection, and linear regression to adjust for confounders and mediators in models assessing direct effects. Factors examined were age, sex, blood pressure, daily smoking, serum lipids, glycated hemoglobin, body mass index (BMI), total body fat percentage (BFP), and the adjustment variables refraction and height.

Results. The explained variance of cardiovascular risk factors was highest in GCIPL (0.126). GCIPL had a strong negative association with age. Women had thicker GCIPL than men at higher age and thinner ORL at all ages ($P < 0.001$). Systolic blood pressure was negatively associated with RNFL/GCIPL ($P = 0.001/0.004$), with indication of a U-shaped relationship with GCIPL in women. The negative association with BMI was strongest in men, with significant effect for RNFL/GCIPL/ORL ($P = 0.001/<0.001/0.019$) and in women for GCIPL/ORL ($P = 0.030/0.037$). BFP was negatively associated with GCIPL ($P = 0.01$). Higher baseline BMI was associated with a reduction in GCIPL over 8 years ($P = 0.03$).

Conclusions. Cardiovascular risk factors explained 12.6% of the variance in GCIPL, with weight and blood pressure the most important modifiable factors.

Keywords: retinal layer thickness, overweight, blood pressure, directed acyclic graphs, covariate adjustment

Optical coherence tomography (OCT) provides noninvasive high-resolution images of the retina.[1,2] It is widely used in clinical practice to evaluate structural changes in retinal disease and glaucoma, and may have a future role in clinical evaluation of neurological diseases.[3,4]

The retina has common embryologic origin with the central nervous system (CNS).[5] It has an anatomic layer structure (Fig. 1), with sensory cells (photoreceptors) in the outer retina, and neurogenic processing and transmitting to the CNS in the middle and inner parts.[6] The vascular supply of the inner retina is through the retinal vessels whose capillary plexuses reaches to the level of the inner nuclear layer, and shares features with the cerebral circulation with a blood-retina barrier and autoregulated flow.[6,7] The outer retina is avascular, and supplied through diffusion from the choroid, a high-flow system which seems not to be metabolic

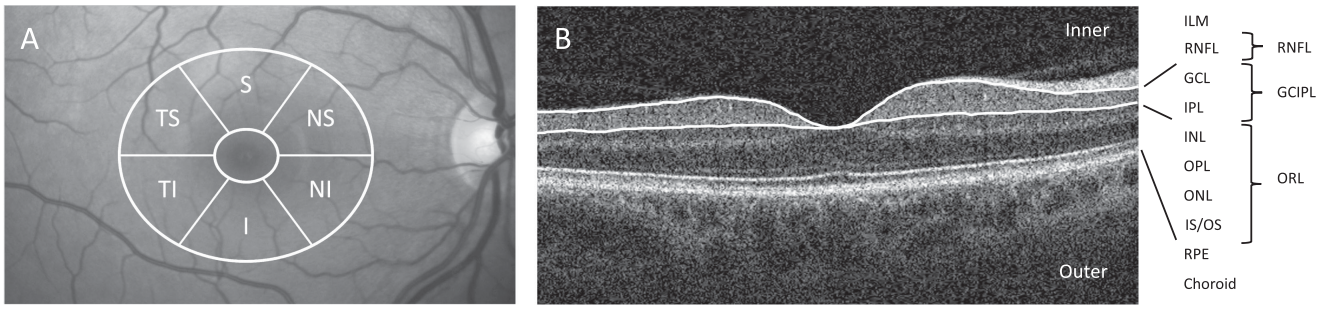

Figure 1. (**A**) OCT image of the macula with the elliptic annulus (dimensions of the inner and outer circle: vertical 1 and 4 mm; horizontal 1.2 and 4.8 mm) around the fovea. TS, temporal superior; S, superior; NS, nasal superior; NI, nasal inferior; I, inferior; TI, temporal inferior. (**B**) Horizontal scan of the macula showing segmentation lines at the outer boundary of retinal nerve fiber layer (RNFL) and the outer boundary of the inner plexiform layer (IPL). The innermost and outermost segmentation lines (not shown) are localized at the level of the internal limiting membrane (ILM) and the retinal pigment epithelium (RPE), respectively. The retina was accordingly segmented in (1) RNFL, (2) ganglion cell-inner plexiform layer (GCIPL) = ganglion cell layer (GCL) + IPL, and (3) outer retinal layers (ORL) = inner nuclear layer (INL) + outer plexiform layer (OPL) + outer nuclear layer (ONL) + photoreceptor inner and outer segments (IS/OS).

controlled, and with the retinal pigment epithelium (RPE) forming the outer blood-retina barrier.[7] The oxygen pressure is highest at the level of the RPE and lowest in the middle retina.[7]

OCT and automated segmentation algorithms allow thickness measurements differentiated on retinal layers.[8,9] As the anatomy, physiology, and vascular supply are layer specific, retinal parts may be differently affected by exposures. The association of age and sex with retinal thickness has been extensively studied, also separated on different retinal layers.[10–18] Few studies have investigated the association with modifiable cardiovascular risk factors. A study on a Chinese population found no significant associations,[14] another on an Asian population found an inverse association with chronic kidney disease only,[17] and in the large sized UK Biobank Study there was an inverse association with body mass index (BMI), alcohol consumption, and diabetes.[15,16]

We aimed to examine the association of retinal layer thickness with the cardiovascular risk factors, age, sex, blood pressure, daily smoking, serum lipids, glycated hemoglobin (HbA1c), BMI, and total body fat percentage (BFP), and the potential adjustment-variables refraction and height. Directed acyclic graphs (DAGs) provide a visual representation of causal assumptions and guided the regression model building.[19,20] The study of the relationship between retinal layer thickness and cardiovascular risk factors may eventually give important insight into disease mechanisms not only in ocular but also in neurological diseases, as the retina shares features with the CNS.[4,21,22]

Methods

Study Sample

The Tromsø Eye Study (TES) is a substudy of the Tromsø Study, a population-based multipurpose longitudinal study in the municipality of Tromsø, Norway. The baseline TES 1 was conducted in 2007 to 2008 within the sixth survey of the Tromsø Study (Tromsø6).[23,24] The TES 2 was conducted in 2015 to 2016 within the seventh survey (Tromsø7). The study population flow chart is shown in Supplementary Figure S1. We included participants who had OCT-scans in at least one of the surveys, without retinal pathology possibly affecting retinal thickness and with scan quality sufficient for thickness-measurements of the macular retina (see below). We used OCT data from one eye, and in the cross-sectional analyses we used data from one survey. In the selection, we gave priority to scans without drusen, TES 1 before 2, and the right eye before the left. BFP data were collected in a subsample and mainly in Tromsø7, and for participants with BFP in Tromsø7 only, we selected data from Tromsø7 in the cross-sectional analyses. We excluded participants with diabetes and/or diagnosed glaucoma in either survey. A total of 8288 participants were included in the cross-sectional analyses. Among these, 2595 participants had eligible scans from the same eye in both surveys and were included in the longitudinal analyses. Informed consent was obtained from all participants. The study adhered to the tenets of the Declaration of Helsinki and was approved by the Data Inspectorate of Norway and Regional Committee for Medical and Health Research Ethics.

Procedures and Definitions

Data on cardiovascular risk factors and medical health were collected from questionnaires, laboratory testing, and physical examinations, briefly described below and details given elsewhere.[23,25] Resting blood pressure was measured three times with an automatic device (Dinamap Vital Signs Monitor, Tampa, FL, USA), and we used the mean of the last two measurements. Weight and height were measured wearing light clothes without shoes, and BMI was calculated as kilograms per square meter. Non-fasting blood samples were obtained by venipuncture, providing serum levels of HbA1c, high-density lipoprotein (HDL), and low-density lipoprotein (LDL) cholesterol. Smoking status was based on self-reported daily smoking, categorized as current, previous, and never. Diabetes was defined as self-reported diabetes and/or HbA1c $\geq$6.5%. Diagnosis of glaucoma was based on self-report. Total body fat and lean mass were estimated by dual-energy X-ray absorptiometry using a Lunar Prodigy device (GE Healthcare, Madison, WI, USA), with enhanced mode post-scan analyses by enCORE (version 17; GE Healthcare),[26,27] and BFP was calculated as fat(g)/(fat(g) + lean(g)) $\times$ 100.

Refraction was measured by a Nidek auto refractor (AR 660A (TES 1)/ARK 560A (TES 2), Nidek Co., LTD., Gamagori, Japan). We included data as spherical equivalent refraction, calculated as spherical power plus half the cylindrical power in diopters. Both pupils were dilated with

tropicamide 0.5% (Chauvin Pharmaceuticals Ltd., Kingston Upon Thames, Surrey, England, UK). OCT scans were taken of both eyes with the spectral-domain Cirrus HD-OCT model 4000 (Carl Zeiss Meditec [CZM], Jena, Germany), using the standard "512 × 128 macular cube" scan protocol. The retinal segmentation procedure was performed by the Cirrus HD-OCT software (v.8.0.0.518 [TES 1]/v.10.0.0.14618 [TES 2], CZM). Measurements were exported as XML files and extracted with the OCT xml reader (v1.5 [TES 1]/v.1.9 [TES 2], CZM). The algorithm automatically detected the outer boundary of the retinal nerve fiber layer (RNFL) and the outer boundary of the inner plexiform layer (see Fig. 1B) in addition to the internal limiting membrane (ILM) and RPE.[8,9] Measurements of the average thickness of RNFL, ganglion cell-inner plexiform layer (GCIPL), and outer retinal layers (ORL) in 6 sectors of the 14.13 mm^2 elliptic annulus centered at the fovea (see Fig. 1A) were exported. We manually evaluated scan placement, segmentation lines (ILM/RPE), and presence of pathology (drusen, pigment epithelial detachment, epiretinal fibrosis, edema, atrophy of RPE or retina, vitreomacular traction, and/or macular hole), using the Cirrus HD-OCT browser (v.5.0 [TES 1]/v.6.8.0.8308 and v.8.1.0.117 [TES 2], CZM).[24] Scans were eligible if (1) no pathology other than drusen, and (2) of good quality, defined as signal strength ≥6 and no defects or errors in the automated lines for ILM and RPE.

Statistical Analyses

We used Stata/MP 16.1 for Mac (StataCorp, College Station, TX, USA) for all statistical analyses. Any P values <0.05 were considered significant. Associations were analyzed by linear regression models with retinal layer thickness as dependent variable, with separate models for RNFL, GCIPL, and ORL. Age and refraction were curvilinear associated with retinal thickness cross-sectionally and were modeled with quadratic terms. Change in thickness by age, mean over the population age span, was obtained by modeling age with linear term only. Interaction with sex was examined cross-sectionally by including cross-products in regression models and data indicated sex differences in the relationship with age and BMI. Sex-specific results were obtained by including the interaction term of sex and the variable of interest and running separate analyses with inversion of the dichotomous definition of the sex variable. We analyzed a cross-sectional prediction model with several known cardiovascular risk factors, presenting results of total explained variance (R^2) and included standardized regression coefficients to facilitate comparison between the different factors. As refraction and axial length may affect the thickness measurements through magnification affecting the size of the scanned area (see Fig. 1A),[28] we used retinal layer thickness predicted from refraction as dependent variable in the prediction models, to obtain the explained variance of the risk factors only. We used DAGs (Supplementary Fig. S2) to visualize the model of the assumptions of the causal pathways between different exposures and retinal layer thickness.[19,20,29] The DAGs guided the regression model choice, to include sufficient adjustment to obtain the direct effect and to avoid inducing bias by opening possible non-causal pathways. "Direct effect" was defined as the effect of an exposure on thickness, not mediated through or confounded by other variables. Age and sex were included in all models and adjustment for refraction was included in direct effect models to account for the magnification effect on thickness measurements. For age and smoking, we have reported results from nearest approximation to direct effect models (as axial length was unavailable), according to recommendation from Tennant et al.,[20] although adjustment for refraction may possibly induce bias in estimates (Supplementary Fig. S3). Direct effect models separate for independent variables of interest (models are specified in the legend of Supplementary Fig. S2) were analyzed cross-sectionally with layer thickness as dependent variable and longitudinally with change in layer thickness from Tromsø6 to Tromsø7 in the same eye as the dependent variable. To explore the association with BMI, we analyzed the association of different weight-related variables in the subsample which had available BFP data, in cross-sectional age/sex-adjusted and direct effect models. Post hoc we explored a possible U-shaped relationship with blood pressure with details described in the Appendix (Supplementary material).[30] We performed sensitivity analysis on the prediction model excluding persons with drusen.

Results

Population characteristics of the cross-sectional sample, total and stratified by sex (4561 women and 3727 men), are presented in Table 1. Age ranged from 38 to 87 years (mean = 61.5 SD 9.9 years), equally distributed between the sexes. Men had higher levels of blood pressure and BMI. A higher proportion of women was current daily smokers (16.7%), whereas a higher proportion of men was daily smokers (65.4%, previous or current). BFP was available in 2842 participants in the cross-sectional sample and women had higher levels than men. Longitudinal retinal thickness data were available in 2595 participants. Characteristics of these two subsamples and correlation between variables in our models are given in the Supplementary Tables S1 and S2.

Cross-Sectional Analyses

The prediction model showed that the set of cardiovascular risk factors explained most variance (R^2 = 12.6%) in GCIPL, whereas minorly in RNFL and ORL, and evaluated by the standardized coefficients, age, sex, BMI, and systolic blood pressure were the factors of most importance (Supplementary Table S3).

Scatterplots and fitted values of retinal layer thickness versus refraction showed a negative relationship with RNFL and a positive with GCIPL and ORL (Fig. 2). Height was positively associated with RNFL and ORL (Table 2). The sex difference in thickness was biggest in ORL and was evident at all ages (Fig. 3). GCIPL was similar in men and women at lower ages, whereas the difference increased slightly over the age span (see Fig. 3). Adjustment for height in the analyses affected the results for all three layers: The thinner ORL in women remained, although attenuated, the magnitude of the thicker GCIPL in women at higher age was increased, and women had slightly thicker RNFL than men at higher age (Table 2).

Retinal thickness was curvilinear associated with age and there was indication of differences between men and women (see Fig. 3). Results for age (mean change over the population age span) for different adjustment models are shown in Table 2. GCIPL was strongest associated with a reduction with age, with a mean change over the age span of −1.16 µm/5 years in men and −0.96 µm/5 years in women

Table 1. Descriptive Characteristics of Participants Included in Cross-Sectional Analysis, Total and by Sex ($N = 8288$)*

	Total					Men					Women					
Variables	***N***	**Mean/%**	**SD/(n)**	**Min**	**Max**	***N***	**Mean/%**	**SD/(n)**	**Min**	**Max**	***N***	**Mean/%**	**SD/(n)**	**Min**	**Max**	***P* Value**
RNFL, µm†	8288	32.7	3.4	12.0	52.0	3727	32.8	3.7	12.0	48.0	4561	32.7	3.3	13.0	52.0	**0.034**
GCIPL, µm†	8288	78.0	7.1	28.0	104.0	3727	77.5	7.5	28.0	104.0	4561	78.4	6.7	32.0	104.0	**<0.001**
ORL, µm†	8288	128.3	8.3	90.0	196.0	3727	129.9	8.2	92.0	196.0	4561	127.0	8.2	90.0	192.0	**<0.001**
Age, y	8288	61.5	9.9	38.0	87.0	3727	61.6	9.9	38.0	87.0	4561	61.4	9.9	38.0	87.0	0.357
Sex, male	8288	45.0	(3727)													
Systolic BP, mm Hg	8266	135.1	21.7	65.0	258.0	3714	136.5	19.4	83.0	221.5	4552	133.9	23.3	65.0	258.0	**<0.001**
Daily smoking	8198					3693					4505					**<0.001**
Never		37.1	(3040)				34.6	(1279)				39.1	(1761)			
Previous		47.3	(3874)				51.0	(1884)				44.2	(1990)			
Current		15.7	(1284)				14.4	(530)				16.7	(754)			
LDL cholesterol, mmol/L	8227	3.7	1.0	0.8	11.4	3708	3.6	1.0	0.8	11.4	4519	3.7	1.0	1.1	8.4	**<0.001**
HDL cholesterol, mmol/L	8227	1.6	0.5	0.4	4.6	3708	1.4	0.4	0.4	4.6	4519	1.7	0.5	0.5	4.4	**<0.001**
HbA1c, %	8187	5.6	0.3	3.9	6.4	3689	5.61	0.3	4.3	6.4	4498	5.59	0.3	3.9	6.4	**0.047**
Body mass index, kg/m^2	8278	27.0	4.2	12.0	50.6	3726	27.4	3.7	17.0	50.6	4552	26.6	4.5	12.0	50.4	**<0.001**
Weight, kg	8279	77.8	14.7	33.9	150.8	3726	85.8	13.0	48.9	150.8	4553	71.2	12.6	33.9	135.7	**<0.001**
Height, cm	8279	169.5	9.2	141.7	201.2	3726	176.8	6.6	147.6	201.2	4553	163.6	6.3	141.7	185.3	**<0.001**
Total body fat mass, kg‡	2842	26.3	8.4	3.3	68.3	1188	24.4	7.7	6.6	52.5	1654	27.6	8.7	3.3	68.3	**<0.001**
Total body fat, %‡	2842	35.2	7.9	10.3	59.6	1188	29.4	5.9	11.0	45.0	1654	39.3	6.4	10.3	59.6	**<0.001**
Refraction (SER), D	8087	0.2	2.1	−13.5	10.5	3635	0.2	2.1	−13.5	10.1	4452	0.2	2.2	−13.2	10.5	0.947
Drusen, yes§	8288	20.5	(1700)			3727	21.7	(807)			4561	19.6	(893)			**0.020**

N = number of subjects; SD = standard deviation; n = number of cases; Min = minimum; Max = maximum; RNFL = retinal nerve fiber layer; GCIPL = ganglion cell-inner plexiform layer; ORL = outer retinal layers; BP = blood pressure; LDL and HDL = low and high density lipoprotein; HbA1c = glycated hemoglobin; SER = spherical equivalent refraction.

* Men: $N = 1527$ from Tromsø6 and $N = 2200$ from Tromsø7, and women: $N = 1996$ with data from Tromsø6 and $N = 2565$ from Tromsø7. Continuous variables presented as mean and standard deviation (SD), categorical variables (sex, daily smoking, and drusen) as percentages (n) of N. The P value for difference between women and men, continuous variables tested by double sided t-test, and smoking by chi-squared test. The P values < 0.05 are in bold.

† Average thickness in 6 sectors of the 14.13 mm^2 elliptic annulus centered at the fovea.

‡ Total body fat mass and percent, estimated by dual-energy X-ray absorptiometry: $N = 576$ from Tromsø6 and $N = 2266$ from Tromsø7.

§ Drusen only, no other pathology.

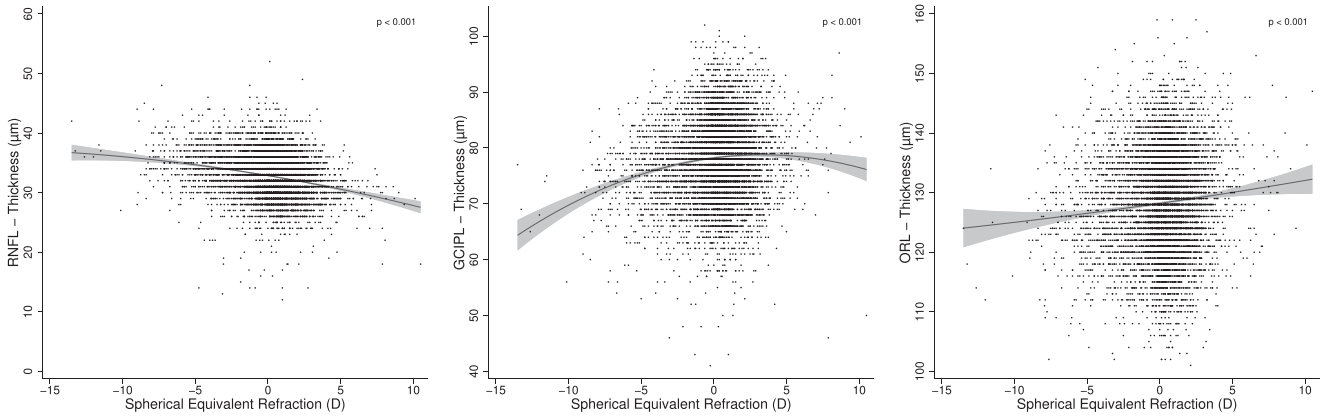

Figure 2. Spherical equivalent refraction and relationship with thickness of the retinal nerve fiber layer (RNFL), ganglion cell-inner plexiform layer (GCIPL), and outer retinal layers (ORLs). Scatterplot and quadratic linear prediction with 95% confidence interval, $N = 8087$. The relationship with RNFL and GCIPL was curved (quadratic term $P = 0.019/<0.001$, respectively).

(both $P < 0.001$). Adjustment for refraction increased the estimates, and corresponding results for the direct effect model was −1.34 µm/5 years in men and −1.17 µm/5 years in women (both $P < 0.001$). RNFL was associated with a slight reduction over the age span, and ORL with a slight increase over the age span in the sex-adjusted model, whereas it was not significant in the direct effect model (see Table 2).

BMI was negatively associated with all three retinal layers in men and GCIPL and ORL in women, with indication of difference in estimates between sexes in RNFL and GCIPL (see Table 2). BFP was negatively associated with GCIPL, whereas not associated with RNFL and ORL (see Table 2). There was no significant difference between women and men in the association with BFP. Supplementary Table S4 shows results for BMI, BFP, weight, and height, stratified by sex, with analyses restricted to the subpopulation with data on BFP and with standardized coefficients to facilitate comparisons.

Systolic blood pressure was negatively associated with RNFL and GCIPL (see Table 2). In women, there was indication of a U-shaped relationship with thinner GCIPL in the group with blood pressure <10 percentile compared to participants with normal blood pressure (Appendix,

Table 2. Retinal Layer Thickness and Association With Height, Sex, Age, and Cardiovascular Risk Factors - Cross-Sectional Analyses With Comparisons of Models*

		RNFL Thickness (µm)		GCIPL Thickness (µm)		ORL Thickness (µm)	
Variable	**Model**	**β (95% CI)**	***P* Value**	**β (95% CI)**	***P* Value**	**β (95% CI)**	***P* Value**
Height/5 cm							
	Age + Sex	0.19 (0.14 to 0.25)	**<0.001**	0.11 (−0.01 to 0.23)	0.066	0.34 (0.20 to 0.49)	**<0.001**
Sex/women†							
at Age = 50 y	Age + Sex	−0.31 (−0.54 to −0.08)	**0.009**	0.45 (−0.01 to 0.90)	0.053	−3.31 (−3.87 to −2.76)	**<0.001**
	Age + Sex + Height	0.19 (−0.09 to 0.47)	0.182	0.74 (0.19 to 1.30)	**0.008**	−2.41 (−3.08 to −1.74)	**<0.001**
	Direct effect model	0.08 (−0.20 to 0.37)	0.571	0.65 (0.10 to 1.21)	**0.022**	−2.83 (−3.52 to −2.13)	**<0.001**
at Age = 65 y	Age + Sex	−0.15 (−0.31 to 0.01)	0.070	0.99 (0.67 to 1.31)	**<0.001**	−2.71 (−3.09 to −2.32)	**<0.001**
	Age + Sex + Height	0.36 (0.13 to 0.58)	**0.002**	1.29 (0.84 to 1.74)	**<0.001**	−1.78 (−2.33 to −1.24)	**<0.001**
	Direct effect model	0.30 (0.08 to 0.53)	**0.009**	1.20 (0.75 to 1.65)	**<0.001**	−2.09 (−2.65 to −1.52)	**<0.001**
Age/5 y‡							
	Age + Sex	−0.23 (−0.27 to −0.19)	**<0.001**	−1.07 (−1.14 to −0.99)	**<0.001**	0.13 (0.03 to 0.22)	**0.007**
	Age + Sex + Height	−0.20 (−0.24 to −0.16)	**<0.001**	−1.04 (−1.12 to −0.97)	**<0.001**	0.18 (0.09 to 0.28)	**<0.001**
	Age + Sex + Height + Refraction	−0.08 (−0.12 to −0.04)	**<0.001**	−1.27 (−1.35 to −1.19)	**<0.001**	0.07 (−0.03 to 0.17)	0.168
	Direct effect model	−0.06 (−0.11 to −0.02)	**0.009**	−1.25 (−1.34 to −1.16)	**<0.001**	0.08 (−0.03 to 0.19)	0.149
Systolic blood pressure/10 mm Hg							
	Age + Sex	−0.08 (−0.12 to −0.04)	**<0.001**	−0.13 (−0.21 to −0.06)	**0.001**	−0.09 (−0.18 to 0.00)	0.063
	Age + Sex + Height	−0.07 (−0.11 to −0.03)	**<0.001**	−0.13 (−0.20 to −0.05)	**0.001**	−0.07 (−0.16 to 0.02)	0.123
	Direct effect model	−0.07 (−0.10 to −0.03)	**0.001**	−0.11 (−0.18 to −0.03)	**0.004**	−0.05 (−0.14 to 0.04)	0.297
Body mass index/5 kg/m^2							
Men	Age + Sex	−0.31 (−0.46 to −0.16)	**<0.001**	−0.52 (−0.81 to −0.22)	**0.001**	−0.52 (−0.88 to −0.15)	**0.005**
	Direct effect model	−0.26 (−0.41 to −0.11)	**0.001**	−0.61 (−0.91 to −0.31)	**<0.001**	−0.45 (−0.83 to −0.08)	**0.019**
Women	Age + Sex	−0.09 (−0.21 to 0.02)	0.099	−0.26 (−0.49 to −0.04)	**0.020**	−0.41 (−0.68 to −0.14)	**0.003**
	Direct effect model	−0.10 (−0.21 to 0.02)	0.110	−0.25 (−0.48 to −0.03)	**0.030**	−0.31 (−0.59 to −0.02)	**0.037**
Total body fat/10 %-point							
	Age + Sex	−0.04 (−0.25 to 0.16)	0.676	−0.58 (−0.99 to −0.18)	**0.005**	−0.18 (−0.67 to 0.32)	0.480
	Age + Sex + Height	−0.03 (−0.24 to 0.17)	0.769	−0.58 (−0.99 to −0.18)	**0.005**	−0.14 (−0.64 to 0.35)	0.570
	Direct effect model	−0.04 (−0.25 to 0.18)	0.745	−0.55 (−0.97 to −0.13)	**0.010**	−0.15 (−0.68 to 0.38)	0.577
Daily smoking, previous vs. never	Direct effect model	−0.09 (−0.25 to 0.07)	0.286	−0.12 (−0.44 to 0.20)	0.468	−0.13 (−0.53 to 0.27)	0.518
Daily smoking, current vs. never	Direct effect model	−0.04 (−0.27 to 0.18)	0.717	−0.00 (−0.44 to 0.44)	0.998	−1.00 (−1.55 to −0.44)	**<0.001**
LDL cholesterol/1 mmol/L	Direct effect model	0.07 (−0.01 to 0.15)	0.079	0.13 (−0.02 to 0.29)	0.089	−0.08 (−0.27 to 0.11)	0.408
HDL cholesterol, 1 mmol/L	Direct effect model	−0.04 (−0.22 to 0.14)	0.662	−0.18 (−0.53 to 0.18)	0.328	0.47 (0.03 to 0.91)	**0.038**
HbA1c/1 %-point	Direct effect model	0.12 (−0.12 to 0.37)	0.323	0.36 (−0.12 to 0.85)	0.142	−0.57 (−1.18 to 0.04)	0.067

RNFL = retinal nerve fiber layer; GCIPL = ganglion cell-inner plexiform layer; ORL = outer retinal layers; β = regression coefficient; CI = confidence interval. LDL and HDL = low and high density lipoprotein; HbA1c = glycated hemoglobin.

* Analysis for height $N = 8279$. For the other variables analyses were restricted to the population with complete variables in the direct effect model to allow comparison between models; sex, age, blood pressure, body mass index, daily smoking, LDL, HDL, and HbA1c: $N = 7864$; total body fat percentage: $N = 2734$. Direct effect models are given in the legend of Supplementary Figure S2. Age and refraction modeled curvilinear and with interaction term sex-age and sex-body mass index when included as adjustment. Interaction with sex, RNFL/GCIPL/ORL, respectively: height $P = 0.34/0.15/0.46$; systolic blood pressure $P = 0.56/0.34/0.75$; body mass index $P = 0.08/0.05/0.53$; total body fat percent $P = 0.98/0.34/0.75$. The P values < 0.05 in bold.

† Due to the curvilinear relationship with age, results are presented for age 50 and 65 years, obtained by separate analyses with age centered at these age values.

‡ Age modeled linearly, change in thickness by age (mean over the population age-span). Age centered at the population mean (Table 1). Results for GCIPL stratified by sex are reported in the text (Results).

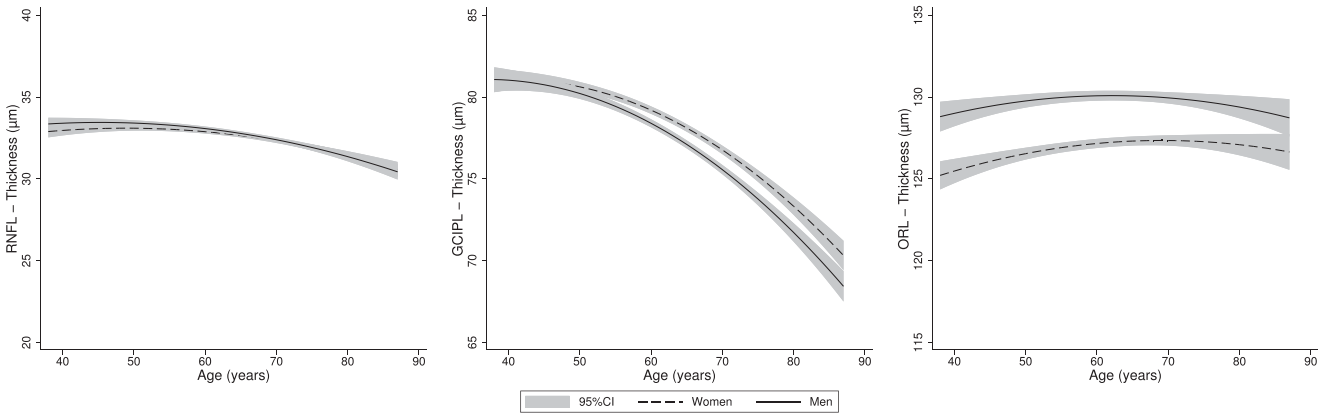

Figure 3. Age and relationship with thickness of the retinal nerve fiber layer (RNFL), ganglion cell-inner plexiform layer (GCIPL), and outer retinal layers (ORL), by sex. Quadratic linear prediction with 95% confidence interval (CI), $N = 8288$. The relationship was curved (quadratic term $P < 0.01$ for all 3 layers). Interaction age sex, level of significance: $P = 0.10$ (RNFL)/0.008 (GCIPL)/0.09 (ORL).

Table 3. Modifiable Cardiovascular Risk Factors and Association with Change in Retinal Layer Thickness from Tromsø6 (2007 to 2008) to Tromsø7 (2015 to 2016) - Longitudinal Analyses, Direct Effect Models ($N = 2460$)[*]

	RNFL Thickness (µm) Change Over 8 Y		GCIPL Thickness (µm) Change Over 8 Y		ORL Thickness (µm) Change Over 8 y	
Variables	**β (95% CI)**	***P* Value**	**β (95% CI)**	***P* Value**	**β (95% CI)**	***P* Value**
Systolic BP/10 mm Hg	−0.04 (−0.07 to 0.00)	0.055	−0.03 (−0.08 to 0.03)	0.381	0.02 (−0.07 to 0.11)	0.630
Daily smoking, previous vs. never[†]	−0.17 (−0.33 to −0.01)	**0.037**	−0.26 (−0.51 to −0.01)	**0.044**	0.27 (−0.12 to 0.67)	0.175
Daily smoking, current vs. never[†]	−0.18 (−0.40 to 0.04)	0.116	−0.37 (−0.71 to −0.03)	**0.034**	0.38 (−0.16 to 0.92)	0.167
LDL cholesterol/1 mmol/L	0.01 (−0.07 to 0.09)	0.875	0.02 (−0.10 to 0.14)	0.743	−0.09 (−0.29 to 0.10)	0.339
HDL cholesterol/1 mmol/L	0.04 (−0.15 to 0.23)	0.667	0.14 (−0.15 to 0.44)	0.339	−0.27 (−0.74 to 0.19)	0.251
HbA1c/1 %-point	0.31 (0.08 to 0.54)	**0.007**	0.13 (−0.22 to 0.49)	0.462	−0.55 (−1.11 to 0.01)	0.052
Body mass index/5 kg/m^2	−0.04 (−0.14 to 0.06)	0.394	−0.17 (−0.32 to −0.01)	**0.033**	−0.11 (−0.36 to 0.13)	0.358

RNFL = retinal nerve fiber layer; GCIPL = ganglion cell-inner plexiform layer; ORL = outer retinal layers; BP = blood pressure; LDL and HDL = low and high density lipoprotein; HbA1c = glycated hemoglobin, β = regression coefficient; CI = confidence interval.

[*] Direct (independent) effect models, according to direct acyclic graphs (DAGs, models specified in the legend of Supplementary Figure S2). No interaction between sex and BMI (*P* values for interaction, RNFL/GCIPL/ORL respectively = 0.6/0.8/0.3). The *P* values <0.05 in bold.

[†] Smoking modeled with nearest approximation to direct effect model (axial length was not available). Total effect model β (µm) *P* values, RNFL/GCIPL/ORL respectively: Smoking, Previous: −0.16 $P = 0.045$/−0.30, $P = 0.017$/0.25, $P = 0.206$. Smoking, current: −0.10 $P = 0.354$/−0.36 $P = 0.031$/0.37 $P = 0.161$.

Supplementary material). HDL was positively and current daily smoking was negatively associated with ORL (see Table 2).

The prevalence of drusen without other pathology was 20.5% (see Table 1), and sensitivity analysis did not indicate that including scans with drusen affected the results (not shown).

Longitudinal Analyses

Mean change in thickness (SD) over 8 years, was RNFL 0.2 (1.8) µm, GCIPL −2.7 (2.8) µm, and ORL 0.5 (4.4) µm, with numbers stratified by sex in the Supplementary Table S1. Higher baseline BMI was associated with a thinning of GCIPL over 8 years, and higher baseline HbA1c with a thickening of RNFL over 8 years (Table 3). Daily smoking at baseline was associated with a thinning over 8 years of RNFL (−0.17 µm, $P = 0.027$) and GCIPL (−0.28 µm, $P = 0.019$), and results separated on previous and current daily smoking are shown in Table 3.

Discussion

In this population-based sample, we found that sex, age, being overweight, and blood pressure were associated with retinal thickness. BMI was negatively associated with all three retinal layers in cross-sectional analyses and with GCIPL in longitudinal analysis. BFP was negatively associated with GCIPL. Blood pressure was negatively associated with RNFL and GCIPL, with an indication of a U-shaped relationship with GCIPL in women.

The GCIPL, which consists of cellular layers of the inner retina, was the layer in which the cardiovascular risk factors explained most variance, and this is in accordance with Khawaja et al.[16] The explained variance of RNFL, mainly consisting of ganglion cell axons, was minor. Both GCIPL and RNFL are circulated by the capillary plexus arising from the retinal vessels which shares features with the cerebral microvascular circulation.[6,7] The explained variance of ORL, which consists of several cellular layers, including the highly metabolic active photoreceptors (see Fig. 1), was minor. This outer part of the retina is mainly supplied by diffusion from the choroid, which differs from the cerebral microvascular circulation.[7] We propose that the shared embryologic origin and vascular structure may indicate that the study of the GCIPL may provide important insight into disease mechanisms in neurologic diseases.

Body size correlates to organ size; large bodies have larger organs. Clinical decision making on cardiovascular dimensions may be confounded by body size.[31] In neuroscience, quantifying direct sex differences in brain regions is complicated by differences in body and head size and is a topic of controversy.[32,33] Body height is positively associated with the ocular size related factors axial length, corneal curvature, and anterior chamber depth.[34,35] The relationship between body height and retinal thickness in adults is scarcely investigated. We found that height was positively associated with RNFL and ORL, corresponding to Yamashita et al. who found that height was positively associated with total retinal thickness in some sectors of the macula in young adults.[36] In contrast, the data from the UK Biobank cohort showed no association between height and retinal thickness in crude analyses.[16] Stature varies significantly by sex and between ethnic groups, and possibly also by age through a cohort-effect due to nutritional status during childhood and adolescence, for which subgroup analysis may be needed.

Corresponding to our results, the UK Biobank study found that BMI was inversely associated with total retinal thickness, RNFL, and GCIPL.[15,16] BMI is commonly used in both clinical settings and research as an indicator for nutritional status, overweight, and obesity. BFP is a more precise indicator of unhealthy weight,[26,37] and a strength of this study was that these data were available in a subsample. BFP was associated with GCIPL only, whereas BMI was associated with all three layers. The interpretation of the relationship between retinal thickness and BMI is complicated by the fact that BMI is defined by height, which in turn is related to eye size and then possibly the retinal thickness. We suspect the association between height versus RNFL and ORL to have an impact on the association between BMI and these two retinal layers. The longitudinal analysis showed that higher baseline BMI was associated with a thinning in GCIPL over 8 years, which supports a causal effect of BMI on GCIPL.

Blood pressure was inversely associated with the inner retinal layers, which is in accordance with previous studies showing thinner inner retinal layers in persons with hypertension.[30,38] Further, we found that women with low blood pressure had thinner GCIPL compared to women with normal blood pressure. This corresponds to results in a recent publication, whereas as noted by the authors, the female proportion in their low blood pressure group was substantially higher than in the reference group with normal blood pressure, and this complicates the interpretation of their results.[30] A strength of our study was that the sample size allowed sex stratified analyses, which seems important exploring this relationship possibly related to glaucoma risk.[39]

In accordance with other studies, our results support that the inverse relationship between age and total macular thickness is mainly due to changes in the inner retinal layers.[10–18] The thicker ORL in men is in accordance with other studies.[12,28] In the present study, we report thinner inner retinal layers in men compared to women. Previous studies have reported inconsistent results, which may in part be related to differences in the age-distributions.[12–14,16,17] Our results indicated that adjustment for height affected the association between retinal thickness and sex. Height-adjusted analyses give results which may be interpreted as sex differences which are independent of the difference in body size between men and women, due to, for example, hormonal effects and sex-related genetics. Adjusted analyses gave that both RNFL and GCIPL were relatively thinner in men than in women with increasing age, and that part of the thicker ORL in men was related to men being taller than women.

The association between refraction and retinal thickness is in concordance with previous studies.[10,13–17,28,36] An ocular magnification effect has theoretical support and Higashide et al. demonstrated it to affect the true size of the scanned area, as in myopia the scanning grid covers a relatively bigger area than in hyperopia, thus includes relatively more of the macular (thinner) periphery.[28] Ooto et al. corrected for the magnification effect on scans upon measurements in their studies and did not find that axial length was associated with total or layer thickness.[11,12] Thus, a possible stretching effect (of a bigger eye) is less likely, at least in the normal range of refractive error/axial length. To reduce a possible effect on estimates due to the magnification effect on thickness measurements, we included adjustment for refraction in the direct effect models and the prediction models.

A strength of our study is the DAGs-guided model-building of adjustment, which illustrates the theoretical assumptions of the causal pathways between exposures and retinal layer thickness, and makes the assumptions transparent and testable.[19,20,40] We acknowledge that this has allowed our models to include "abundant" adjustment (i.e. included factors that do not reach statistical significant level or do not [substantially] change estimates of the effect of the factor of interest). This opposed to data-driven strategies for model building in which the final adjustment model may be dependent on and sensitive to the specific data and order of decisions, thus more susceptible to bias-inducing adjustment. Variable selection according to the level of significance in univariate analyses may result in lack of variables in the model that, for example, differ in distribution or effect between sexes, or variables that differ with age. Moreover, it may lead to biased results by improper adjustment. We consider it essential to explore possible sex-differences in data and associations and to run sex-specific analyses where appropriate. It remains to be explored to what extent allometric scaling by body size and the magnification effect of ocular refraction on retinal thickness measurements in general are of importance for causal inference concerning ocular and neuronal changes and disease.

We included persons with drusen to avoid healthy participant bias, as the prevalence of drusen is high in a middle- and old-age population. Glaucoma was based on self-report, which is a limitation, as the prevalence of glaucoma is higher than of diagnosed glaucoma. Another possible limitation is that our DAGs may be too simple, either lacking causal pathways between model variables or lacking variables not included in the model but related to both retinal thickness and other variables in the diagram.

Even with longitudinal data, as our study includes, the prerequisite of temporality (exposure precedes the effect) shares limitations with cross-sectional analyses, as change in a factor is related to the baseline value. Still, causal inference is a fundamental question in science,[41] and drawing causal inference from observational data presumes plausible theoretical assumptions behind the statistical models. The longitudinal data on BMI, the use of BFP as a measure of being overweight. and the DAGs guided regression model building adds to our knowledge on the association of BMI with retinal thickness. Together they provide support that overweight and obesity cause thinning of the cellular layers of the inner retina.

Acknowledgments

Supported by the Northern Norway Regional Health Authority (SFP1262-15), Dr. Jon S. Larsens Foundation and Arthur og Odd Clausons Legat. The sponsor or funding organization had no role in the design or conduct of this research. The author(s) have no proprietary or commercial interest in any materials discussed in this article.

Disclosure: **T. von Hanno**, None; **L.L. Hareide**, None; **L. Småbrekke**, None; **B. Morseth**, None; **M. Sneve**, None; **M.G. Erke**, None; **E.B. Mathiesen**, None; **G. Bertelsen**, None

References

1. Huang D, Swanson EA, Lin CP, et al. Optical coherence tomography. *Science.* 1991;254:1178–1181.
2. Kiernan DF, Mieler WF, Hariprasad SM. Spectral-domain optical coherence tomography: a comparison of modern high-resolution retinal imaging systems. *Am J Ophthalmol.* 2010;149:18–31.
3. Chen J, Lee L. Clinical applications and new developments of optical coherence tomography: an evidence-based review. *Clin Exp Optom.* 2007;90:317–335.
4. Snyder PJ, Alber J, Alt C, et al. Retinal imaging in Alzheimer's and neurodegenerative diseases. *Alzheimers Dement.* 2021;17:103–111.
5. Fuhrmann S. Eye morphogenesis and patterning of the optic vesicle. *Curr Top Dev Biol.* 2010;93:61–84.
6. Cuenca N, Ortuño-Lizarán I, Sánchez-Sáez X, et al. Interpretation of OCT and OCTA images from a histological approach: Clinical and experimental implications. *Prog Retin Eye Res.* 2020;77:100828.
7. Pournaras CJ, Rungger-Brändle E, Riva CE, Hardarson SH, Stefansson E. Regulation of retinal blood flow in health and disease. *Prog Retin Eye Res.* 2008;27:284–330.
8. Giani A, Cigada M, Choudhry N, et al. Reproducibility of retinal thickness measurements on normal and pathologic eyes

by different optical coherence tomography instruments. *Am J Ophthalmol.* 2010;150:815–824.
9. Mwanza J-C, Oakley JD, Budenz DL, Chang RT, Knight ORJ, Feuer WJ. Macular ganglion cell-inner plexiform layer: automated detection and thickness reproducibility with spectral domain-optical coherence tomography in glaucoma. *Invest Ophthalmol Vis Sci.* 2011;52:8323–8329.
10. von Hanno T, Lade AC, Mathiesen EB, Peto T, Njølstad I, Bertelsen G. Macular thickness in healthy eyes of adults (N = 4508) and relation to sex, age and refraction: the Tromsø Eye Study (2007–2008). *Acta Ophthalmol.* 2017;95:262–269.
11. Ooto S, Hangai M, Sakamoto A, et al. Three-dimensional profile of macular retinal thickness in normal Japanese eyes. *Invest Ophthalmol Vis Sci.* 2010;51:465–473.
12. Ooto S, Hangai M, Tomidokoro A, et al. Effects of age, sex, and axial length on the three-dimensional profile of normal macular layer structures. *Invest Ophthalmol Vis Sci.* 2011;52:8769–8779.
13. Mwanza J-C, Durbin MK, Budenz DL, et al. Profile and predictors of normal ganglion cell-inner plexiform layer thickness measured with frequency-domain optical coherence tomography. *Invest Ophthalmol Vis Sci.* 2011;52:7872–7879.
14. Koh VT, Tham Y-C, Cheung CY, et al. Determinants of ganglion cell-inner plexiform layer thickness measured by high-definition optical coherence tomography. *Invest Ophthalmol Vis Sci.* 2012;53:5853–5859.
15. Patel PJ, Foster PJ, Grossi CM, et al. Spectral-Domain Optical Coherence Tomography Imaging in 67 321 Adults: Associations with Macular Thickness in the UK Biobank Study. *Ophthalmology.* 2016;123:829–840.
16. Khawaja AP, Chua S, Hysi PG, et al. Comparison of Associations with Different Macular Inner Retinal Thickness Parameters in a Large Cohort: The UK Biobank. *Ophthalmology.* 2020;127:62–71.
17. Tham YC, Chee ML, Dai W, et al. Profiles of Ganglion Cell-Inner Plexiform Layer Thickness in a Multi-Ethnic Asian Population: The Singapore Epidemiology of Eye Diseases Study. *Ophthalmology.* 2020;127:1064–1076.
18. Ramyashri S, Rao HL, Jonnadula GB, et al. Determinants of Optical Coherence Tomography Parameters in a Population-based Study. *Am J Ophthalmol.* 2021;224:163–171.
19. Textor J, van der Zander B, Gilthorpe MS, Liskiewicz M, Ellison GT. Robust causal inference using directed acyclic graphs: the R package 'dagitty'. *Int J Epidemiol.* 2016;45:1887–1894.
20. Tennant PWG, Murray EJ, Arnold KF, et al. Use of directed acyclic graphs (DAGs) to identify confounders in applied health research: review and recommendations. *Int J Epidemiol.* 2021;50:620–632.
21. Feigl B. Age-related maculopathy - linking aetiology and pathophysiological changes to the ischaemia hypothesis. *Prog Retin Eye Res.* 2009;28:63–86.
22. Mursch-Edlmayr AS, Bolz M, Strohmaier C. Vascular Aspects in Glaucoma: From Pathogenesis to Therapeutic Approaches. *Int J Mol Sci.* 2021;22:4662.
23. Jacobsen BK, Eggen AE, Mathiesen EB, Wilsgaard T, Njølstad I. Cohort profile: The Tromso Study. *Int J Epidemiol.* 2012;41:961–967.
24. Bertelsen G, Erke MG, von Hanno T, et al. The Tromsø Eye Study: Study design, methodology and results on visual acuity and refractive errors. *Acta Ophthalmol.* 2013;91:635–642.
25. von Hanno T, Bertelsen G, Sjølie AK, Mathiesen EB. Retinal vascular calibres are significantly associated with cardiovascular risk factors: the Tromsø Eye Study. *Acta Ophthalmol.* 2014;92:40–46.
26. Messina C, Albano D, Gitto S, et al. Body composition with dual energy X-ray absorptiometry: from basics to new tools. *Quant Imaging Med Surg.* 2020;10:1687–1698.
27. Johansson J, Strand BH, Morseth B, Hopstock LA, Grimsgaard S. Differences in sarcopenia prevalence between upper-body and lower-body based EWGSOP2 muscle strength criteria: the Tromsø Study 2015-2016. *BMC Geriatr.* 2020;20:461.
28. Higashide T, Ohkubo S, Hangai M, et al. Influence of Clinical Factors and Magnification Correction on Normal Thickness Profiles of Macular Retinal Layers Using Optical Coherence Tomography. *PLoS One.* 2016;11:e0147782.
29. Textor J. DAGitty — draw and analyze causal diagrams, http://www.dagitty.net/; Online launch August 2021-March 2022, version 3.0 2019.
30. Pappelis K, Jansonius NM. U-Shaped Effect of Blood Pressure on Structural OCT Metrics and Retinal Perfusion in Ophthalmologically Healthy Subjects. *Invest Ophthalmol Vis Sci.* 2021;62:5.
31. Dewey FE, Rosenthal D, Murphy DJ, Jr., Froelicher VF, Ashley EA. Does size matter? Clinical applications of scaling cardiac size and function for body size. *Circulation.* 2008;117:2279–2287.
32. Sanchis-Segura C, Ibañez-Gual MV, Aguirre N, Cruz-Gómez ÁJ, Forn C. Effects of different intracranial volume correction methods on univariate sex differences in grey matter volume and multivariate sex prediction. *Sci Rep.* 2020;10:12953.
33. Williams CM, Peyre H, Toro R, Ramus F. Neuroanatomical norms in the UK Biobank: The impact of allometric scaling, sex, and age. *Hum Brain Mapp.* 2021;42:4623–4642.
34. Wei S, Sun Y, Li SM, et al. Effect of body stature on refraction and ocular biometry in Chinese young adults: The Anyang University Students Eye Study. *Clin Exp Optom.* 2021;104:201–206.
35. Yamashita T, Iwase A, Sakai H, Terasaki H, Sakamoto T, Araie M. Differences of body height, axial length, and refractive error at different ages in Kumejima study. *Graefes Arch Clin Exp Ophthalmol.* 2019;257:371–378.
36. Yamashita T, Tanaka M, Kii Y, Nakao K, Sakamoto T. Association between retinal thickness of 64 sectors in posterior pole determined by optical coherence tomography and axial length and body height. *Invest Ophthalmol Vis Sci.* 2013;54:7478–7482.
37. Müller MJ, Braun W, Enderle J, Bosy-Westphal A. Beyond BMI: Conceptual Issues Related to Overweight and Obese Patients. *Obes Facts.* 2016;9:193–205.
38. Lim HB, Lee MW, Park JH, Kim K, Jo YJ, Kim JY. Changes in Ganglion Cell-Inner Plexiform Layer Thickness and Retinal Microvasculature in Hypertension: An Optical Coherence Tomography Angiography Study. *Am J Ophthalmol.* 2019;199:167–176.
39. Flammer J, Orgül S, Costa VP, et al. The impact of ocular blood flow in glaucoma. *Prog Retin Eye Res.* 2002;21:359–393.
40. Schisterman EF, Cole SR, Platt RW. Overadjustment bias and unnecessary adjustment in epidemiologic studies. *Epidemiology.* 2009;20:488–495.
41. Hernán MA. The C-Word: Scientific Euphemisms Do Not Improve Causal Inference From Observational Data. *Am J Public Health.* 2018;108:616–619.

Investigative Ophthalmology & Visual Science